HHS Public Access

Author manuscript

Breast Cancer Res Treat. Author manuscript; available in PMC 2017 January 12.

Published in final edited form as:

Breast Cancer Res Treat. 2016 January ; 155(2): 235–251. doi:10.1007/s10549-015-3673-z.

The TRAIL Receptor Agonist Drozitumab Targets Basal B Triple Negative Breast Cancer Cells that Express Vimentin and Axl

Jennifer L. Dine[1,2,3], **Ciara C. O'Sullivan**[1], **Donna Voeller**[1], **Yoshimi E. Greer**[1], **Kathryn J. Chavez**[1], **Catherine M. Conway**[4], **Sarah Sinclair**[5], **Brandon Stone**[1], **Laleh Amiri-Kordestani**[1], **Anand S. Merchant**[6], **Stephen M. Hewitt**[4], **Seth M. Steinberg**[7], **Sandra M. Swain**[5], and **Stanley Lipkowitz**[1]

[1]Women's Malignancies Branch, Center for Cancer Research, National Cancer Institute, National Institutes of Health, Bethesda, MD

[2]Intramural Research Program, National Institute of Nursing Research, National Institutes of Health, Bethesda, MD

[3]Sinclair School of Nursing, University of Missouri, Columbia, MO, USA

[4]Laboratory of Pathology, Center for Cancer Research, National Cancer Institute, National Institutes of Health, Bethesda, MD

[5]Washington Cancer Institute, MedStar Washington Hospital Center, Washington, DC.

[6]Center for Cancer Research Bioinformatics Core, Advanced Biomedical Computing Center, SAIC-Frederick, Frederick, MD

[7]Biostatistics & Data Management Section, Center for Cancer Research, National Cancer Institute, National Institutes of Health, Bethesda, MD 20892, USA

Abstract

Purpose—Previously, we found that GST-tagged tumor necrosis factor-related apoptosis inducing ligand (TRAIL) preferentially killed triple negative breast cancer (TNBC) cells with a mesenchymal phenotype by activating death receptor 5 (DR5). The purpose of this study was to explore the sensitivity of breast cancer cell lines to drozitumab, a clinically tested DR5 specific agonist; identify potential biomarkers of drozitumab-sensitive breast cancer cells; and determine if those biomarkers were present in tumors from patients with TNBC.

Methods—We evaluated viability, caspase activity, and sub-G1 DNA content in drozitumab-treated breast cancer cell lines and we characterized expression of potential biomarkers by immunoblot. Expression levels of vimentin and Axl were then explored in 177 TNBC samples from a publically available cDNA microarray dataset and by immunohistochemistry (IHC) in tumor tissue samples obtained from 53 African American women with TNBC.

Corresponding Author: Stanley Lipkowitz, M.D., Ph.D., Women's Malignancies Branch, Center for Cancer Research, National Cancer Institute, National Institutes of Health,, Building 10, Room 4B54, Phone: (301) 402-4276; Fax: (301) 402-4275;, lipkowis@mail.nih.gov.

Competing Interests

The authors declare they have no competing interests.

Results and Conclusions—Drozitumab induced apoptosis in mesenchymal TNBC cell lines but not in cell lines from other breast cancer subtypes. The drozitumab-sensitive TNBC cell lines expressed the mesenchymal markers vimentin and Axl. Vimentin and Axl mRNA and protein were expressed in a subset of human TNBC tumors. By IHC, ~15% of TNBC tumors had vimentin and Axl expression in the top quartile for both. These findings indicate that drozitumab-sensitive mesenchymal TNBC cells express vimentin and Axl, which can be identified in a subset of human TNBC tumors. Thus, vimentin and Axl may be useful to identify TNBC patients who would be most likely to benefit from a DR5 agonist.

Introduction

Breast cancer is a heterogeneous group of diseases that may be stratified into subtypes based on the presence of distinct molecular markers [1]. Approximately 60-70% of breast cancers are estrogen receptor (ER) or progesterone receptor (PR) positive, and 15-30% of cases have amplification and overexpression of the human epidermal growth factor receptor 2 (HER2) protein [2]. Additionally, 10-15 % of breast cancers are termed "triple negative" due to the absence of ER and PR expression and *HER2* amplification [2]. Most triple negative breast cancers (TNBC) are characterized by an aggressive presentation and inferior survival outcomes, especially in the relapsed or metastatic setting [3-5]. The TNBC subset is over represented in African American women and accounts, in part, for the worse outcomes in this group [3,4]. Unlike the treatment strategies available for ER and/or PR expressing or *HER2* amplified subsets of breast cancer, effective targeted therapies have yet to be developed for TNBC. In the absence of a targeted therapy with which it may be combined, chemotherapy is currently the standard of care for this patient population [6]. There is a clear need to develop effective, targeted therapies for TNBC.

Extensive characterization has revealed remarkable diversity in the molecular attributes of TNBC [7-10]. The majority of TNBC is basal-like, which is characterized by elevated expression of keratins 5/6 and 17, *TP53* mutation, aberrations in DNA repair pathways (e.g., *BRCA1* loss), and pro-proliferative gene expression [7]. Pre-clinically, basal-like TNBC cell lines have been further segregated into basal A (epithelial) and basal B (mesenchymal) subtypes [9]. While the basal A subtype retains a more epithelial phenotype, the basal B subtype possesses stem cell-like characteristics and also preferentially expresses specific markers, including the intermediate filament protein vimentin and receptor tyrosine kinase Axl [9]. Subsequent studies have explored using vimentin [11-14] or Axl [15] as TNBC/basal-like biomarkers in human breast tumors. Vimentin has been a particularly robust biomarker for TNBC, and vimentin and Axl have been associated with poor prognosis [11-15].

Previously, we determined that basal B TNBC cell lines were the most sensitive breast cancer subtype to tumor necrosis factor (TNF)-related apoptosis inducing ligand (TRAIL) while breast cancer cell lines representative of the other subtypes of the disease remained comparatively resistant [16]. TRAIL induces apoptosis via ligand binding to the death receptors, DR4 and 5 (*a.k.a.* TRAIL receptor 1 and TRAIL receptor 2, respectively), which results in the formation of the death inducing signaling complex (DISC) and recruitment and activation of caspase-8 [17]. In some cells, the mitochondrially-mediated apoptotic pathway

may also be activated downstream of DR activation by caspase-8 mediated cleavage of Bid, resulting in mitochondrial outer membrane permeabilization, apoptosome formation, and caspase-9 activation [17]. Both caspases-8 and -9 are then able to directly activate the executioner caspases-3/7, culminating in apoptosis [17]. Interestingly, TRAIL has been found to be highly specific in selecting for transformed cells, resulting in little or no toxicity to normal cells *in vitro* and little toxicity *in vivo* [18,19]. The available clinical evidence suggests that TRAIL receptor agonists, either as monotherapy or in combination with other agents, are generally well-tolerated but exert limited efficacy in unselected patient populations [20-25]. Thus, further drug development of TRAIL receptor agonists will require predictive biomarkers to identify subsets of patients with tumors most likely to respond to these agents.

Given the preclinical observation that basal B TNBC cells are sensitive to TRAIL [16], we have sought to specifically investigate the sensitivity of breast cancer cell lines to drozitumab [26], a monoclonal DR5-specific TRAIL-receptor agonist antibody, and to explore the expression levels of biomarkers that may correlate with sensitivity, including vimentin and Axl. We then aimed to investigate the expression levels of those biomarkers in publically available cDNA microarray data sets and by immunohistochemistry (IHC) in breast cancer tissues derived from African-American women. The goal of this study is to evaluate sensitivity to drozitumab in cell lines representative of the different subtypes of breast cancer (*i.e.*, ER positive, HER2 amplified, and TNBC), identify biomarkers of sensitivity to drozitumab, and characterize expression of those biomarkers in human breast cancer.

Materials and Methods

Cell Culture

The HCC1937, BT20, and MB157 cell lines were obtained from Reinhard Ebner (Avalon Pharmaceuticals, Germantown, MD). The MCF7, ZR75-1, T47D, MB453, SKBR3, HCC1953, MB468, HCC38, HS578t, and MB231 cell lines were obtained from American Type Culture Collection (Manassas, VA, USA). All cancer cell lines were grown in RPMI 1640 base media plus 10% fetal calf serum, 100 units/ml of penicillin, and 100 units/ml of streptomycin. Primary non-transformed HMEC1 cells were obtained from Lonza (Cat # CC-2551, Basel, Switzerland) and grown in the HMEC media (Cat # 3150) obtained from Lonza. hTERT-HME1 cells were generously provided by Jeffery Green at National Cancer Institute and maintained in the same media as the primary HMEC cells.

Inhibitors

Z-VAD-FMK, a pan-caspase inhibitor (Cat # P416, Biomol International, Plymouth Meeting, PA), was reconstituted in DMSO and used at 100 μM concentration. Drozitumab, a monoclonal DR5 agonist antibody, and the vehicle control [0.5 M arginine succinate, 20 mM Tris, 0.02% Tween 20 (pH 7.2)], were kindly provided by Dr. Avi Ashkenazi (Genentech, Inc., South San Francisco, CA).

siRNA transfections

A pool of siRNAs for Axl (Cat # L-003104-00-0005), vimentin (Cat # L-003551-00-0005), and a matched non-targeting control (Cat # D-001810-10-20) were obtained from Dharmacon (Thermo Fisher Scientific, Waltham, MA). A pool of siRNAs for DR4 (Cat # 1027417 - SI00056728), DR5 (Cat # 1027417 - SI03094063), and a matched non-targeting control (Cat # 1027281) were obtained from Qiagen (Valencia, CA). MB231 cells were plated on 10 cm tissue culture dishes and grown in RPMI supplemented with 10% FBS for 48 h prior to transfection. Reverse transfections were performed by incubating siRNA's at a final concentration of 33 nM in 7.5 ml of Opti-MEM media (Thermo Fisher Scientific, Grand Island, NY) with 37.5 μl of Lipofectamine RNAiMax transfection reagent (Cat # 13778-150, Thermo Fisher Scientific, Grand Island, NY). After a 20 min incubation at RT for complex formation between the RNAiMax and the siRNA, cells (1.5 mls at 1.0×10^6 cells/ml in RPMI supplemented with 10% FCS) were added to the siRNA mix and distributed to 96 well plates with a final cell concentration of 5,000 cells/well. Cells for immunoblot analysis were distributed to 6 well plates at 500,000 cells/well. The cells were incubated for 48 h. After 48 h cells were either treated with GST-TRAIL or drozitumab. For GST-TRAIL treatment experiments, GST-TRAIL was added to transfected cells at a final concentration of 0, 250, and 1,000 ng/ml. For MTS assays cells were incubated with GST-TRAIL for 24 h for the Axl and vimentin siRNA tranfections and 72 hours for the DR4 and DR5 siRNA transfections. For caspase-3/7 assays, cells were incubated with GST-TRAIL for 1 h. For drozitumab treatment, F(ab')2 fragment goat anti-human IgG (Cat # 109-006-098, Jackson Immunoresearch, West Grove, PA) was added to the cells at a final concentration of 10,000 ng/ml. Immediately following F(ab')2 addition, drozitumab was added to the transfected cells at a final concentration of 0, 2500, and 10,000 ng/ml. Control cells were treated with F(ab')2 alone + drozitumab vehicle at 10,000 ng/ml. Cells were incubated with drozitumab for 72 h for the MTS assays, for 24 h for caspase-3/7 assays, and for 3 h for caspase-8 assays.

Viability Assay

Cells were plated overnight in 96 well plates and then treated under the experimental conditions described in the body of the text. Viability was subsequently determined using the CellTiter 96 AQueous One Solution Cell Proliferation Assay (Cat # G3582, Promega Corporation, Madison, WI) as previously described [16]. At least three independent experiments were carried out and included six replicates per experiment. Results are provided as the mean +/− SE of at least three independent experiments.

Caspase-Glo® assays

Cells were treated GST-TRAIL or drozibumab as indicated in the text and figure legends. For caspase inhibition, cells were preincubated with 100 uM ZVAD-FMK or DMSO for two hours and subsequently incubated overnight with 2500 ng/ml drozitumab or 2500 ng/ml drozitumab plus 10 μg/ml F(ab')2. Caspase activity was assessed using the Caspase-Glo® 3/7 assay system (Cat # G8092, Promega Corporation, Madison, WI) and/or Caspase-Glo® 8 assay system (Cat # G8202, Promega Corporation, Madison, WI) as previously described [27]. Three independent experiments normalized to the control cells +/− SE were performed.

Lysate Preparation and Immunoblotting

Cell lysate preparation and immunoblotting were performed as previously described [16]. Rabbit monoclonal antibodies to Axl (Cat # 4566, Cell Signaling, Beverly, MA) and ER alpha (Cat # 8644, Cell Signaling, Beverly, MA); rabbit polyclonal antibodies to DR4 (Cat # GTX28414, GenTex, Inc, Irvine, CA), DR5 (Cat # 2019 , ProSci Inc, Poway, CA), ERBB2 (Cat # Rb103P0, Thermo Scientific, Pittsburgh, PA) and PARP (Cat # 7150, Santa Cruz Biotechnology, Dallas, TX); and mouse monoclonal antibodies to β-actin (Cat # A5316, Sigma-Aldrich, St. Louis, MO), caspase-8 (Cat # 9746, Cell Signaling, Beverly, MA), HSP70 (Cat # 7298, Santa Cruz Biotechnology, Dallas, TX), E-cadherin (Cat # 610181, BD Biosciences Pharmingen, San Jose, CA), tubulin (Cat #T9026, Sigma, St. Louis, MO), and vimentin (Cat # 550513, BD Biosciences Pharmingen, San Jose, CA) were used for immunoblotting.

DISC analysis

To examine drozitumab induced recruitment of caspase-8 to DR5, cells were incubated with drozitumab (10 μg/ml) + goat anti-human Fc IgG (10 μg/ml; Cat # 109-001-008, Jackson Immunoresearch, West Grove, PA) or with the anti-human Fc IgG alone for 30 min. Cells were lysed as described above, and DR5 was precipitated by adding Protein A/G PLUS-agarose beads (Cat. # 2003, Santa Cruz Biotechnology, Dallas, TX) to the lysate. For the cells that had been incubated without drozitumab, drozitumab and antihuman-IgG were added after the cells were lysed in amounts equal to the amount added prior to lysis of the cells in the drozitumab treated cells. The cell lysates were tumbled with the agarose A/G beads overnight and then washed 5 times with lysis buffer. The pellet was resuspended in loading buffer and analyzed by immunoblotting as previously described [16].

To examine GST-TRAIL induced recruitment of caspase-8 to DR5, cells were incubated with or without GST-TRAIL at 500 ng/ml for 15 min. Cells were lysed and as described above, and DR5 precipitated by adding agarose agarose-glutathione (agarose-GSH) beads (Cat # sc-2009, Santa Cruz Biotechnology, Dallas, TX) to the lysate. For the cells that had been incubated without GST-TRAIL, GST-TRAIL was added after the cells were lysed in amounts equal to the amount added prior to lysis of the cells in the GST-TRAIL treated cells. The cell lysates were tumbled with the agarose-GSH beads overnight, and then washed 5 times with lysis buffer. The pellet was resuspended in loading buffer and analyzed by immunoblotting.

The immunoblots for these DR5 immunoprecipitations were developed on an Odyssey-Fc imaging system (LI-COR Biosciences, Lincoln, NE) and directly quantitated based on the digital images.

Sub-G1 Analysis

MB231 cells were plated overnight and subsequently treated with 2500 ng/ml drozitumab, 2500 ng/ml drozitumab plus 10 μg/ml F(ab')2, or equal volumes of drozitumab vehicle or drozitumab vehicle plus F(ab')2. Cell harvesting, propidium iodide staining, flow cytometry method, and data analysis technique were described previously [28]. Three independent experiments normalized to the vehicle-treated control +/− SE were performed.

Analysis of Publically Available Microarray Data

A single merged superset of 696 samples was created from collating publicly available breast cancer datasets (GSE2034, GSE3494 and GSE 1456) that were conducted on the same microarray platform (Affymetrix Human Genome HGU133A). Based on available clinical metadata, this superset comprised of 484 ER positive, 177 ER negative (or TNBC), and 15 ERBB2/Her2 positive patients. Twenty patients did not have information (NA). Normalized log-transformed expression values for vimentin and Axl genes were extracted for the 177 TNBC samples, and median centering along with euclidean clustering was applied to generate the heatmap (Fig 4a). Spearman's correlation analysis was used to statistically assess the correlation between expression of Vimentin and Axl in this subset of TNBC samples.

Immunohistochemistry

Immunohistochemistry (IHC) stains for vimentin and Axl were performed on slides prepared from tumor blocks from patients with TNBC diagnosed at MedStar Washington Hospital Center, Washington, D.C. between February 2003 and February 2009. The study at MedStar Washington Hospital Center was approved by the appropriate Institutional Review Board. Tumor samples analyzed by IHC at NIH were unlinked from patient identifiers and the protocol was reviewed by the NIH Office of Human Subjects Research and determined to be exempt from IRB approval.

Slides were deparaffinized in xylene and rehydrated in graded alcohols. Antigen retrieval was performed in a pressure cooker for 20 minutes with citrate buffer (pH 9). Primary antibody was incubated at room temperature for 2 hours, and antibody-antigen reaction detected with Dako Envision+ secondary and DAB (Dako, Carpinteria CA). Primary antibodies were vimentin (mouse monoclonal, clone V9, Dako, Carpinteria, CA) at 1:4000 dilution and Axl (rabbit polyclonal, Cat # ab72069, Abcam, Cambridge MA) at 1:100 dilution. Slides were dehydrated in grade alcohols, cleared in xylene and coverslipped.

Slides were imaged with a Hamamatsu Nanozoomer HT (Hamamatsu, Bridgewater , NJ) at 20X resolution. Images were uploaded to SlidePath DIH (Leica, Dublin, Ireland) for annotation and image quantification. Tumor cells were identified and annotated for quantification by inspection. Quantification was performed with TIA, within SlidePath DIH, using a cytoplasmic staining algorithm to quantify DAB intensity. For Axl the average intensity was normalized for the final output. For vimentin, a threshold intensity was defined, and the number of positive pixels/total number of pixels was used as a surrogate for percent cells staining as the final output. The correlation between the expression of vimentin and Axl protein was determined by Spearman correlation.

Statistical Methods for Analysis of Clinical Parameters

This was a retrospective cohort study. A retrospective search was carried out in the database of all women diagnosed with invasive breast cancer at Washington Hospital Center between February 2003 and February 2009. Eligible patients were females aged ≥ 18 years, of African-American ethnicity, with a confirmed pathological diagnosis of stage I-IV TNBC. Patient characteristics included age at diagnosis, date of diagnosis, stage, and laterality of

disease. Treatment characteristics included the type of surgery (breast conserving vs. mastectomy), chemotherapy (yes/no), radiotherapy (yes/no), and whether or not patients declined or did not complete chemotherapy and/or radiotherapy. The primary outcomes were disease free survival (DFS) and overall survival (OS). Cause of death was determined from the electronic patient record. The potential observation time was from the date of diagnosis until the date of death or end of available follow-up information, as recently as April 16, 2014. All information was collected on Excel spreadsheets and stored in password-protected files in accordance with the Health Insurance Portability & Accountability Act (HIPAA) guidelines. The data were cleaned and de-identified. Analyses were performed by a statistician (SMS) in the Biostatistics and Data Management Section of the National Cancer Institute (NCI). The study was approved by the IRB at Georgetown University prior to its initiation.

Fifty-three patients with TNBC were included in analyses to determine the association of Axl and vimentin with clinical outcomes. OS was calculated from date of surgery until date of death or last follow-up. DFS was calculated from the date the patient was identified as being free of disease (at the first or subsequent surgery) until the date of recurrence or date last followed without a recurrence. Patients without a known date of surgery were excluded from analyses, as were patients who were not able to be identified as having a definite date in which they were found to be disease free. Patients for whom it was not able to be determined if they had a recurrence were excluded from the DFS analyses.

The significance of the difference among Kaplan-Meier curves was determined by a log-rank test. Axl, vimentin, and age at diagnosis values were divided approximately into quartiles based on data from all available TNBC patients before being used in actuarial analyses. The groupings thus result in approximate effects and, to the extent they suggest trends, may be refined in subsequent confirmatory analyses.

In general, p-values are reported unadjusted for multiple comparisons because they are all considered to be exploratory. However, when patients were analyzed initially by grouped Axl, vimentin, or age values and the results suggested that a preferred, dichotomous division in the groupings would indicate a better prognostic association with the outcome, the resulting p-values were adjusted by multiplying by the implicit number of such comparisons performed to identify the final grouping. A Cox proportional hazards model analysis was also performed to determine if Axl or vimentin retained prognostic value after adjusting for other factors which were jointly associated with outcome. All p-values are two-tailed.

Results

Drozitumab Induces Apoptosis in Breast Cancer Cells

In our prior work using a recombinant GST-TRAIL fusion protein, we found that the basal B TNBC cells are sensitive to TRAIL-induced apoptosis while other subtypes of breast cancer cells were relatively resistant [16]. GST-TRAIL can activate both DR4 and DR5. To test whether both DR4 and DR5 contributed to GST-TRAIL induced apoptosis in breast cancer cells we transfected the MB231 cell line with siRNAs for DR4, DR5, or both and then assessed the effects of GST-TRAIL on caspases-3 and -7 activation and viability (Fig.

1a-c). GST-TRAIL induced an 8-10 fold increase in activation of caspases-3/7 and significantly decreased viability (Fig. 1a and b, respectively, white bars). Knockdown of DR5 significantly decreased caspases-3/7 activation and rescued the viability of the GST-TRAIL treated cells compared to cells transfected with a negative siRNA (siNEG) control (Fig. 1a and b respectively, compare the striped bars to the white bars). By contrast, knockdown of DR4 had only a small effect on GST-TRAIL mediated caspase 3/7 activation or loss of viability compared to the siNEG control (Fig. 1a and b respectively, compare the grey bars to the white bars). Knockdown of both DR4 and DR5 resulted in less caspase activation than the knockdown of either alone but only resulted in a significant decrease at the 1000 ng/ml concentration of GST-TRAIL (Fig. 1a compare black bars to the striped bars). The knockdown of both DR4 and DR5 resulted in a small, non-statistically significantly rescue of viability compared to siDR5 alone (Fig. 1b, compare black bars to the striped bars). Thus the data show that DR5 is the major mediator of GST-TRAIL induced caspase activation and loss of viability. However DR4 does contribute to GST-TRAIL-induced caspase activation and to a lesser extent to the loss in viability. This is consistent with our previous findings in multiple breast cancer cell lines that DR5 is required for GST-TRAIL induced death of breast cancer cells whereas DR4 was not required for GST-TRAIL induced death [16]. Thus, to confirm the findings that the basal B TNBC are most sensitive to TRAIL receptor agonists that activate DR5, we evaluated the ability of drozitumab (a fully human anti-DR5 specific TRAIL receptor agonist [26]) to kill breast cancer cells. We first tested drozitubmab for activity on the TRAIL sensitive, basal B TNBC MB231 cell line. MB231 was treated for 1 and 5 days with vehicle; 10 ug/mL of anti-human IgG cross-linking fragment antigen binding region (F(ab')2); drozitumab alone; vehicle plus10 ug/mL of F(ab')2; and drozitumab plus 10 ug/mL of F(ab')2. MTS assays were then used to assess cell viability (Fig. 1d). Crosslinking drozitumab with F(ab')2 has been reported to potentiate DISC formation, caspases-8 and -3/7 activation, and cell death compared to drozitumab alone [26]. We found that drozitumab +/−F(ab')2 killed cells in a dose-dependent manner but that crosslinking drozitumab with F(ab')2 decreased viability more rapidly and potently than drozitumab alone. The IC50 of drozitumab plus F(ab')2 after 1 day was ~10 ug/mL, and the IC50 after 5 days was ~300ng/mL. By contrast, drozitumab alone did not result in any loss in viability at 1 day post treatment, and the IC50 was ~625ng/mL after 5 days.

To confirm that drozitumab toxicity depended on DR5 and not on DR4, we measured caspase activation and viability of the cells treated with drozitumab after siDR4, siDR5, or siDR4 and siDR5 (Fig. 1e and f). Drozitumab induced a 2-3 fold increase in activation of caspases-3/7 and significantly decreased viability (Fig. 1e and f, respectively, white bars). Knockdown of DR5 completely abrogated drozitumab-induced caspase activation and loss of viability compared to siNEG (Fig 1e and f, compare the striped bars to the white bars). Knockdown of DR4 had no effect on either caspase activation or loss of viability induced by drozitumab compared to siNEG (Fig 1e and f, compare grey bars to white bars). The knockdown of both DR4 and DR5 was not different from the knockdown of DR5 alone (Fig 1e and f, compare black bars to the striped bars). Thus drozitumab-induced caspase activation and loss of viability is mediated solely by DR5.

Cleavage of pro-caspase-8 into a mature and active product [29] is one of the earliest steps of TRAIL-stimulated DR5 signaling. Once activated, caspase-8 will cleave and activate

other caspases, including the executioner caspases-3/7, to carry out the apoptotic program [17]. To investigate the effects of drozitumab on DR5-mediated caspase activation, we measured the cleavage of pro-caspase-8 over time after treatment with drozitumab +/−F(ab')2. We also measured in parallel the cleavage of PARP, a caspases-3/7 substrate whose cleavage is a hallmark of apoptosis (Fig. 2a) [30]. The loss of the precursors and the appearance of cleaved product for both caspase-8 and PARP were more rapid and greater for drozitumab + F(ab')2 than for drozitumab alone. Drozitumab + F(ab')2 was able to robustly induce cleavage of caspase-8 and PARP after 30 minutes of treatment while drozitumab alone required 1 hour of treatment to attain comparable levels of cleavage (Fig. 2a). At later time points (*i.e.*, 2-8 hours) the loss of the precursors was greater in cells treated with drozitumab + F(ab')2 than it was for drozitumab alone, consistent with greater activation of the DR5 receptor by the F(ab')2-crosslinked drozitumab (Fig. 2a). These findings are consistent with earlier studies indicating that the addition of F(ab')2 to drozitumab more rapidly induced caspase activation than drozitumab alone [26]. The dependence of drozitumab mediated toxicity on caspase activation was further explored by measuring caspases-3/7 activity and viability in MB231 cells in the presence or absence of pre-treatment with the pan-caspase inhibitor ZVAD-FMK (Figs. 2b and c respectively). Caspase activation was measured using a luminescent caspases-3/7 assay (Fig. 2b). Drozitumab induced an ~2.5 fold increase in caspases-3/7 activity, compared to vehicle alone (Fig. 2b). F(ab')2 crosslinked drozitumab induced an ~3 fold increase in caspases -3/7 activity compared to vehicle treated cells (Fig. 2b). F(ab')2 alone did not induce any caspases-3/7 activity compared to vehicle treated cells (data not shown). The addition of the pan-caspase inhibitor ZVAD-FMK completely blocked the increase in caspases-3/7 activity induced by drozitumab or F(ab')2 crosslinked drozitumab (Fig. 2b). In parallel experiments, pretreatment of the cells with ZVAD-FMK completely rescued the viability of the cells treated with either drozitumab or F(ab')2 crosslinked drozitumab (Fig. 2c). Together these findings demonstrate that drozitumab or F(ab')2 crosslinked drozitumab promotes caspase-dependent loss of viability in the cells.

To confirm that drozitumab induces apoptotic cell death, sub-G_1 DNA content was measured in MB231 cells treated with drozitumab or drozitumab + F(ab')2 for 48 hours. Drozitumab and F(ab')2 crosslinked drozitumab substantially increased the percentage of cells with sub-G1 DNA content by 4-5 fold compared to their respective controls (Fig. 2d). F(ab')2 crosslinked drozitumab did not induce significantly different levels of sub-G1 cells and in fact the percentages were overall slightly lower. This could reflect a more rapid cell death kinetic in the cells treated with F(ab')2 crosslinked drozitumab, resulting in fewer cells with sub-G1 content at 48 hours.

In summary, drozitumab induces caspase-dependent apoptotic cell death. Activation of the apoptotic machinery is more rapidly and potently activated with the addition of the F(ab')2 cross-linking agent to drozitumab.

Drozitumab preferentially kills basal B TNBC cells

We have previously shown that cell lines that represent TNBC with mesenchymal features (basal B TNBC cells) are the most sensitive to GST-TRAIL-induced apoptosis [16]. To

explore the sensitivity of breast cancer cells to drozitumab a panel of 14 breast cancer cell lines representative of the different subtypes of disease were treated with drozitumab +/− F(ab')2 for 5 days. Viability was then measured by MTS assay (Fig. 3a). Drozitumab induced loss of viability in every basal B TNBC cell line tested (HCC38, HS578t, MB157, and MB231), and F(ab')2 crosslinking of dozitumab increased the loss of viability (Fig. 3a). Drozitumab with or without crosslinking did not induce loss of viability in the ER positive, HER2 amplified, and the basal A TNBC cell lines (Fig. 3a). In parallel, we assessed the expression of protein markers to confirm the phenotype of the cells (Fig. 3a, immunoblot shown below bar graph). Expression of ER and HER2 confirmed the identification of cells as ER positive, HER2 amplified, or TNBC. To further characterize the basal A and basal B subsets of the TNBC, expression of E-cadherin, vimentin, and Axl were measured. E-cadherin is expressed in epithelial cells and vimentin is expressed in mesenchymal cells [31]. Axl is highly expressed in mesenchymal breast cancer cells [16,32] . The basal B TNBC all expressed vimentin (Fig. 3a, lanes 11-14), whereas none of the other cell lines expressed vimentin. Axl was expressed in all of the basal B TNBC and in the basal A TNBC HCC1937 (Fig. 3a, lanes 11-14). E-cadherin expression was found in the basal B TNBC HCC38 cell line but not in any of the other basal B TNBC cell lines. E-cadherin was expressed in all of the basal A TNBC and ER positive cell lines (Fig. 3a lanes 1-3 and 8-10). The only HER2 amplified cell line that expressed E-cadherin is the HCC1954 cell line. The viability data and the immunoblots suggest that a subset of TNBC that express the mesenchymal markers vimentin and Axl are the most sensitive to drozitumab-induced loss of viability.

We next investigated the effects of drozitumab on non-transformed human mammary epithelial cells (Fig. 3b-c). We tested drozitumab induced caspase activation and loss of viability in primary non-immortalized human mammary epithelial cells (HMEC1) derived from reduction mammoplasty and a telomerase immortalized, non-transformed HMEC (hTERT-HME1). Drozitumab induced inhibition of viability in both HMEC1 and hTERT-HME1, although to a lesser extent that in the HS578t basal B breast cancer cell line (Fig.3b). Like the basal B breast cancer cell lines (Fig. 3a) both HMEC1 and hTERT-HME1 expressed vimentin and Axl (Fig. 3c, lanes 1 and 2, top two panels). E-cadherin was expressed at a low level in HMEC1 and at a high level in hTERT-HME1 (Fig. 3c, lanes 1 and 2, third panel). Variable expression of E-cadherin was also seen in the basal B breast cancer cell lines (Fig. 3a, see HCC38 vs the other basal B cell lines). Both HMEC1 and hTERT-HME1 had low levels of Her-2 expression and did not express estrogen receptor (Fig. 3c, lanes 1 and 2, fouth and fifth panel). Thus the two non-transformed lines phenotypically resemble the basal B breast cancer cell lines and are sensitive to drozitumab.

Axl negatively regulates drozitumab-induced caspase activation and loss of viability

To investigate the role of vimentin and Axl in drozitumab induced caspase activation and cell death, we transfected the basal B MB231 cell line with siRNAs targeting either vimentin or Axl (Fig. 4). Knockdown of vimentin did not significantly affect either drozitumab-induced caspases-3/7 activation or loss of viability compared to the siNEG control (Fig. 4 a-b, compare the black bars to the grey bars). By contrast knockdown of Axl resulted in greater drozitumab-induced activation of caspases-3/7 and loss of viability compared to

siNEG (Fig. 4 a-b, compare the striped bars to the grey bars). Similar effects of Axl and vimentin knockdown were shown for caspases-3/7 activation by GST-TRAIL (Supplementary Fig. 1a). A representative immunoblot of the siRNA knockdown of vimentin and Axl is shown in Fig. 4c. We next looked at the activity of the initiator caspase-8 and found that knockdown of Axl significantly increased drozitumab induced caspase-8 activation compared to siNEG control (Fig. 4d, compare the striped bars to the grey bars). The knockdown of vimentin did not significantly affect drozitumab-induced caspase-8 activation (Fig. 4d, compare the black bars to the grey bars). A representative immunoblot of the siRNA knockdown of vimentin and Axl is shown in Fig. 4e. Thus, Axl negatively regulates drozitumab induced caspase activation and loss of viability while vimentin does not regulate either ligand induced caspase activation or cell death.

To investigate whether Axl affected the formation of the death-inducing signaling complex (DISC) induced by drozitumab, we measured the recruitment of caspase-8 to DR5 upon drozitumab treatment. DR5 precipitated from cells treated with drozitumab + anti-Fc antibody co-precipitated caspase-8 precursor and the cleaved activated forms while DR5 from untreated cells did not (Fig. 4f, compare lanes 4 and 6 to lanes 3 and 5, respectively). To quantify these bands, we measured the intensity of the sum of the caspase-8 precursor and cleaved caspase-8 bands divided by the intensity of the sum of the two DR5 bands in the DR5 precipitations all normalized to the cells treated with the non-targeting siRNA (siNEG). The ratio of caspase-8/DR5 was higher in the cells in which Axl was knocked down compared to those treated with siNEG (Fig 4f, see numbers below lanes 4 and 6). A similar result was seen in cells activated by GST-TRAIL (Supplementary Fig 1b). The ratio of caspase-8/DR5 was higher in GST-TRAIL activated DR5 pulldowns from cells in which Axl was knocked down (Supplementary Fig. 1b, see numbers below lanes 5 and 7). Across four experiments there was a consistent increase in the ratio of caspase-8/DR5 when Axl was knocked down with an average relative change of 1.73 fold+/−0.22 (Supplementary Fig. 1c). Thus it appears that Axl inhibits drozitumab and GST-TRAIL induced caspase activation and cell death at least in part by negatively regulating caspase-8 recruitment to DR5. A previously published study described Axl mediated inhibition of caspase-8 activation by interaction with DR5 at the DISC [33]. We did not see any co-immunoprecipiation of Axl with DR5 (Fig. 4f; lanes 3-6 and supplementary Fig 1b, lanes 4-7).

Vimentin and Axl are expressed in human TNBC

In order to characterize vimentin and Axl expression in TNBC tumors, we investigated transcriptional and protein expression levels from human TNBC tumors. mRNA expression of vimentin and Axl was evaluated in TNBC tumor biopsies from 177 patients derived from three merged publically available cDNA microarray data sets that utilized the same microarray platform for analysis (Fig. 5a) [34-36]. Of the 177 TNBC samples, ~43% and ~41% samples had high mRNA expression of vimentin and Axl, respectively. Approximately 39% of TNBC samples expressed high levels of both vimentin and Axl mRNA. The expression of vimentin and Axl showed strong correlation in the TNBC samples from these merged data sets ($r= 0.6$; $p<0.0001$). These findings confirm that vimentin and Axl are transcriptionally expressed in a subset of human TNBC breast tumors.

The mRNA expression of vimentin and Axl in tumors described above could be in either the tumor cells or the stroma. In order to demonstrate that expression of vimentin and/or Axl was in the tumor cells, we performed IHC in TNBC samples from a cohort of 53 African-American women that were treated over a 6 year period (February 2003-February 2009) at Washington Hospital Center in Washington, D.C. (Table 1). The median age at diagnosis was 56 years (range: 31-72). The majority of patients had either stage II or III disease at diagnosis (n=46; 86.8%), and most patients received chemotherapy (n=50; 94.3 %). A substantial proportion of patients received neoadjuvant chemotherapy (n=21; 39.6 %). Approximately one-third of participants (16/53=30.1%) declined or did not complete chemotherapy, a finding which is likely related to complex socio-economic factors in this patient demographic.

We assessed staining of vimentin and Axl in the tumor cells by IHC. Vimentin was quantified based on the percentage of tumor cells positive for vimentin staining. The range of staining was from 0-49% of cells staining positive for vimentin. The top quartile samples showed vimentin staining in 15-49% of tumor cells. Axl was quantified based on the intensity of staining with the top quartile of samples showing a Axl score of 0.575-1.00 in the tumor. Thus a subset of TNBC can be identified that express vimentin, Axl, or both. We were able to identify vimentin and Axl expression in the tumor cells and differentiate between expression in tumor and stroma. We observed combinations of low Axl and low vimentin , high Axl and low vimentin, low Axl and high vimentin , and high Axl and high vimentin in the tumor cells (Fig. 5b). The expression of vimentin and Axl protein was only weakly correlated in the IHC data set (r=0.29; p=0.035) (Fig. 6). However, approximately 15% of tumors expressed high levels of both vimentin and Axl (as defined by expression in the top quartile for both). These findings demonstrate that a subset of TNBC with high vimentin and Axl protein are identifiable using IHC.

We reviewed all of the cases to identify adjacent normal terminal ductal-lobular units (TDLUs). We identified three cases with normal TDLUs, for which all three demonstrated positive epithelial and myoepithelial staining for Axl but negative staining in the stroma (supplementary Fig. 2). The three cases demonstrated positive stromal and myoepithelial staining for vimentin but no epithelial cell staining within the TDLUs (supplementary Fig. 2). This is consistent with staining patterns of Axl and vimentin reported in the literature for normal breast tissue [37,38].

We explored DFS and OS in this cohort of patients with TNBC. DFS and OS were superior in patients with stage I or II disease compared to that of patients with stage III or IV disease. The 5 year DFS probabilities were 79.0% (95% Confidence Interval (CI): 61.0-90.0%) for stage I and II vs. 26.7% (95% CI: 8.4-59.0%) for stage III and IV (p=0.0006). The 5 year OS probabilities were 75.4% (95% CI: 57.2-87.0%) for stage I and II vs. 60.2 % (95% CI: 35.7-80.5%) for stage III and IV (p=0.024). Of the 21 patients who received neoadjuvant chemotherapy, 2 achieved a pathological complete response (pCR), 16 responded, and 3 progressed on therapy. Those patients that achieved a pCR or responded to neoadjuvant chemotherapy had a significantly better OS (5 year OS probability of 74.7%, with 95% CI: 49.8-89.7%) compared to those who progressed on therapy (all three died, at 15.1, 18.5, and 22.3 months; adjusted p=0.01).

Following exploratory analyses, good separation of Kaplan-Meier curves for DFS and OS was obtained by splitting the data into the top quartile vs. the lower 3 quartiles of both vimentin (values >0.1455 vs. <=0.1455 and Axl staining (values >0.669 vs. <=0.669). These results are shown in Fig. 7a and 7b for vimentin and Axl respectively. High vimentin expression (defined as the top quartile) showed a trend towards an association with improved DFS and a significantly better OS by univariate analysis than those whose tumors had lower vimentin expression (Fig. 7a). High Axl expression showed weak association with DFS or OS by univariate analysis (Fig. 7b).

Among these patients with TNBC, the following parameters were associated with at least a trend towards significance with respect to DFS in univariate analyses: Axl (<0.669 vs. >0.669); vimentin (<=0.1455 vs. >0.1455); age (29-55 vs. >55); stage (I,II vs. III, IV); neoadjuvant treatment (none, not applicable vs. yes); and response to neo-adjuvant therapy (progression vs. anything else: PCR, residual, not applicable). Response to neo-adjuvant therapy was excluded from further consideration for models. Since the best division only consisted of 3 patients with progression with the rest in a combined category, the generalizability of the parameter was limited. Using backward elimination, Cox multivariable analysis led to a model showing that vimentin >0.1455 was associated with superior DFS (p=0.046) when adjusting for age and stage (Table 2a). For OS, Axl (<0.330 vs. >=0.330—the median value, selected for the Cox model because it had slightly better univariate prognostic value than did 0.669), vimentin (<=0.1455 vs. >0.1455), stage (I,II vs. III, IV), and response to neo-adjuvant therapy (progression vs. anything else: PCR, residual, not applicable) were factors found to be potentially associated with OS in univariate analyses. By backward elimination, Cox model analysis showed that vimentin >0.1455 was associated with lower probability of dying (p=0.026) when adjusting for stage, the only other potential prognostic factor remaining in the model (Table 2b).

Discussion

The results presented here demonstrate that the DR5 receptor agonist drozitumab induces caspase dependent apoptosis in basal B TNBC but not in cells from other subtypes of breast cancer (Figs. 1, 2 & 3). The addition of cross-linking F(ab')2 to drozitumab more rapidly and potently induced loss in viability than drozitumab treatment alone, consistent with previous findings [26]. Crosslinking of drozitumab, mediated by leukocyte Fc gamma receptor expression, is required for activity of drozitumab *in vivo* [39]. The killing of basal B TNBC by drozitumab is concordant with our previous data demonstrating that a recombinant form of the natural ligand, GST-TRAIL, selectively induced apoptosis in basal B TNBC through activation of DR5 [16]. Thus, both recombinant TRAIL and an agonist antibody to DR5 induced apoptosis in this subset of breast cancer cells. While both DR4 and DR5 can be activated by the GST-TRAIL ligand used in our prior study, DR5 is the predominant death receptor activated by GST-TRAIL in breast cancer cells (Fig. 1a-c) [16]. The basis for the DR5 selectivity of GST-TRAIL is unclear but could be due to either absolute expression levels of DR5 vs. DR4 or the relatively higher affinity of DR5 for TRAIL [40]. The results using drozitumab, a specific DR5 agonist, are consistent with our previous observation that TRAIL receptor agonists which activate DR5 induce apoptosis in the basal B TNBC cells.

TRAIL receptor agonists, including drozitumab, have been tested either alone or in combination with other agents in phase I and II clinical trials. Little clinical benefit has been observed to date [20]. This has led to discontinuation of the development of these agents in many cases. However, none of the clinical trials stratified patients based on potential predictive biomarkers of response, and none specifically evaluated activity in TNBC. In our work, all of the cell lines express either DR4 and DR5, and we did not find any correlation between TRAIL sensitivity and DR4 or DR5 total or surface protein level expression [16,41]. One study of pancreatic cancer, colorectal cancer, non-small-cell lung cancer, and melanoma cell lines identified low expression of O-glycosylation genes as a potential mechanism of TRAIL-resistance [42]. In our previous analysis of the breast cancer cell lines we did not find a correlation between the expression of genes for O-glycosylation and TRAIL sensitivity [16,41]. Lu *et al.* demonstrated that epithelial to mesenchymal transition in non-small cell lung cancer cells attenuated DR4 and DR5 apoptotic signaling and further that E-cadherin directly interacts with DR4 and DR5 to facilitates DISC assembly and caspase-8 activation in response to TRAIL in lung, colon, and pancreatic cancer cell lines [43]. However, our findings indicate that the majority of basal B TNBC cell lines express low levels of E-cadherin, express mesenchymal markers such as vimentin and Axl, and are most sensitive to TRAIL (Fig. 3) [16]. These findings suggest there may be tissue-specific differences regarding sensitivity to TRAIL, requiring the identification of biomarkers relevant to each tissue type [44,39].

Transcriptional profiling of the breast cancer cell lines has identified two subsets of basal TNBC, so called basal A and basal B cells [9]. These cell types differed in expression of either epithelial (basal A) or mesenchymal (basal B) genes. Both our previous work and the current data found that the basal B TNBC cells were selectively killed by TRAIL receptor agonists. These cell lines all expressed the mesenchymal markers vimentin and Axl. The majority of the basal B TNBC cell lines that we tested in this work (Fig. 3) and in our previous work [14] cluster with molecular subtypes of TNBC identified by expression analyses that are characterized by mesenchymal features, including the claudin-low TNBC [45] and mesenchymal stem like TNBC [10]. Mesenchymal markers, including high vimentin and low E-cadherin expression are included in the definition of these subtypes and so our findings are consistent with these classifications [45,10]. The claudin low TNBC represent ~25-39% of TNBC, and the mesenchymal stem like TNBC represent ~15% of TNBC [30, 31]. However, not all of the basal B cell lines are classified as claudin low or mesenchymal stem cell like. The HCC38 cell line, for example, clusters with the basal TNBC in both of these analyses, and the BT549 characterized in our previous study clusters with mesenchymal like cells in the analysis by Lehmann *et al.* [30, 31]. Thus the expression of vimentin and Axl identify a broader group of TNBC that may be sensitive to TRAIL receptor agonists than is identified as claudin low or as mesenchymal stem like.

We investigated whether vimentin or Axl were mechanistically related to the sensitivity to TRAIL receptor agonists in the basal B cell lines. siRNA mediated knock down of vimentin had no effect on drozitumab or GST-TRAIL induced caspase activation or induction of cell death (Fig. 4, supplementary Fig. 1a). This is consistent with our previously published findings [16]. Thus vimentin, while a marker of the breast cancer cells that are most

sensitive to TRAIL receptor agonists, is not mechanistically the cause of the cells sensitivity TRAIL receptor agonists.

siRNA mediated knock down of Axl had a paradoxical effect. While Axl is expressed in the cells most sensitive to TRAIL receptor agonists, the knock down of Axl led to increased sensitivity to drozitumab and GST-TRAIL induced caspase activation and loss of viability (Fig. 4, supplementary Fig. 1). Mechanistically, we found a modest increase in association of caspase-8 with DR5 when Axl was knocked down (Fig. 4f and supplementary Fig. 1b). Similarly, a study by Hong and Belkhiri demonstrated that Axl inhibited TRAIL-mediated caspase activation and death in esophageal adenocarcinoma cells by inhibiting caspase-8 recruitment to the DISC [33]. Using cells stably overexpressing Axl, they were able to demonstrate that Axl co-precipitated with DR5. We did not find any association of Axl with DR5 in our studies (Fig 4f and supplementary Fig. 1b). This could be due to differences in the cell types studied or to lower sensitivity in our work using endogenous proteins. The mechanism by which Axl inhibits DISC formation in the breast cancer cells will require further study.

Nontransformed mammary epithelial cells (HMEC1 and hTERT-HME1) expressed Axl and vimentin like the basal B breast cancer cells and were sensitive to drozitumab-induced loss of viability (Fig. 3b-c). Most non-transformed breast cell lines have basal features and most closely resemble the basal B cancer cell lines [46]. The normal breast tissue showed distinct patterns of staining for vimentin (predominantly stromal) and Axl (predominantly in the duct epithelial cells) (Supplementary Fig. 2). This is consistent with previous descriptions of the localization of these proteins [37,38]. Interestingly both vimentin and Axl stained the myoepithelial cells (Supplementary Fig. 2). Myoepithelial cells are most similar to the basal breast cancer cells [8] so that the coincidence of vimentin and Axl staining in these cells is concordant with the expression of both in the basal B breast cancer cell lines. There have been no reports of any overt breast toxicity and no studies have assessed whether there is any loss of myoepithelial cells in the breast from patients treated with TRAIL receptor agonists.

mRNA and protein expression of vimentin and Axl was found in TNBC tumors and approximately 15% of the TNBC have high levels of both proteins by IHC (Fig. 5a, b and 6). While the molecular mechanisms that regulate TRAIL sensitivity in breast cancer remain elusive [41,16], vimentin and Axl expression identified a subset of TNBC that express one or the other of these mesenchymal markers (Figs. 3, 5a and 5b). Although vimentin expression has been found to consistently be associated with TNBC [14,13,12,11], one study found that Axl expression, while associated with aggressive disease, did not segregate with TNBC but was found across ER negative and ER positive subtypes [15]. Thus, vimentin may be a more selective marker for the basal B TNBC. Since only a small fraction of the TNBC would be identified by co-expression of vimentin and Axl (~15% with high levels of both), an unstratified clinical trial would have a majority of the TNBC that are predicted to be resistant to TRAIL receptor agonists and thus more likely to show no benefit to these agents. Thus, vimentin and Axl expression could be used to stratify patients in a clinical trial to test whether our preclinical observations also predict responses to TRAIL receptor agonists in patients.

In an exploratory analysis of the relationship of vimentin and Axl expression to outcomes in 53 African American women, Axl, vimentin, stage, and response to neoadjuvant chemotherapy were factors found to be potentially associated with OS in univariate analyses while Axl, vimentin, age, neoadjuvant chemotherapy, response to neoadjuvant chemotherapy, and stage were associated with at least trends towards significance with respect to DFS in univariate analyses.

Improved outcomes were associated with early stage and response to neoadjuvant chemotherapy. This latter finding reflects chemosensitivity in TNBC tumors [47]. In the evaluated cohort, high expression of vimentin was associated with improved DFS and OS (Fig. 7 and Table 2). This finding contradicts published data showing either association of vimentin with worse outcomes with DFS and OS outcomes in this setting. Published data have generally found vimentin expression to be associated with basal and TNBC phenotype, and generally most publications have found worse outcomes or no association with outcome associated with vimentin [11-15,48]. Our finding of improved outcome could be due to the small sample size or unknown or unmeasured patient characteristics. Interestingly, the majority of the patients received chemotherapy, many in the neoadjuvant setting. Thus, our findings could indicate that the TNBC that express vimentin are particularly sensititive to chemotherapy compared to other TNBC. Our lab previously demonstrated that combining TRAIL and chemotherapy results in increased cytotoxicity in breast cancer cells [49]. Thus, combining TRAIL receptor agonists with chemotherapy may be useful in patients with TNBC and particularly in those TNBC which express vimentin and/or Axl.

Our data, combined with the existing evidence, demonstrates that the TNBC cell lines which express mesenchymal markers (*i.e.*, vimentin and Axl) are most sensitive to TRAIL receptor agonists. IHC identifies TNBC tumors with mesenchymal features. Therefore IHC for vimentin and Axl could be used in clinical trials to select patients with TNBC who may derive benefit from TRAIL receptor agonists. Together, these data suggest that TRAIL receptor agonists targeted to basal B TNBC should be explored further in clinical trials.

Supplementary Material

Refer to Web version on PubMed Central for supplementary material.

Acknowledgements

This research was supported by the Intramural Research Program of the National Cancer Institute, Center for Cancer Research and MedStar Health Research Institute supported by a grant from the Safeway Foundation.

References

1. Prat A, Perou CM. Deconstructing the molecular portraits of breast cancer. Mol Oncol. 2011; 5(1): 5–23. doi:10.1016/j.molonc.2010.11.003. [PubMed: 21147047]
2. Brenton JD, Carey LA, Ahmed AA, Caldas C. Molecular classification and molecular forecasting of breast cancer: ready for clinical application? J Clin Oncol. 2005; 23(29):7350–7360. doi:10.1200/JCO.2005.03.3845. [PubMed: 16145060]
3. Morris GJ, Naidu S, Topham AK, Guiles F, Xu Y, McCue P, Schwartz GF, Park PK, Rosenberg AL, Brill K, Mitchell EP. Differences in breast carcinoma characteristics in newly diagnosed African-American and Caucasian patients: a single-institution compilation compared with the

National Cancer Institute's Surveillance, Epidemiology, and End Results database. Cancer. 2007; 110(4):876–884. doi:10.1002/cncr.22836. [PubMed: 17620276]

4. Carey LA, Perou CM, Livasy CA, Dressler LG, Cowan D, Conway K, Karaca G, Troester MA, Tse CK, Edmiston S, Deming SL, Geradts J, Cheang MC, Nielsen TO, Moorman PG, Earp HS, Millikan RC. Race, breast cancer subtypes, and survival in the Carolina Breast Cancer Study. JAMA. 2006; 295(21):2492–2502. doi:10.1001/jama.295.21.2492. [PubMed: 16757721]
5. Millikan RC, Newman B, Tse CK, Moorman PG, Conway K, Dressler LG, Smith LV, Labbok MH, Geradts J, Bensen JT, Jackson S, Nyante S, Livasy C, Carey L, Earp HS, Perou CM. Epidemiology of basal-like breast cancer. Breast Cancer Res Treat. 2008; 109(1):123–139. doi:10.1007/s10549-007-9632-6. [PubMed: 17578664]
6. Perou CM. Molecular stratification of triple-negative breast cancers. Oncologist. 2011; 16(Suppl 1): 61–70. doi:10.1634/theoncologist.2011-S1-61. [PubMed: 21278442]
7. Cancer Genome Atlas N. Comprehensive molecular portraits of human breast tumours. Nature. 2012; 490(7418):61–70. doi:10.1038/nature11412. [PubMed: 23000897]
8. Perou CM, Sorlie T, Eisen MB, van de Rijn M, Jeffrey SS, Rees CA, Pollack JR, Ross DT, Johnsen H, Akslen LA, Fluge O, Pergamenschikov A, Williams C, Zhu SX, Lonning PE, Borresen-Dale AL, Brown PO, Botstein D. Molecular portraits of human breast tumours. Nature. 2000; 406(6797):747–752. doi:10.1038/35021093. [PubMed: 10963602]
9. Neve RM, Chin K, Fridlyand J, Yeh J, Baehner FL, Fevr T, Clark L, Bayani N, Coppe JP, Tong F, Speed T, Spellman PT, DeVries S, Lapuk A, Wang NJ, Kuo WL, Stilwell JL, Pinkel D, Albertson DG, Waldman FM, McCormick F, Dickson RB, Johnson MD, Lippman M, Ethier S, Gazdar A, Gray JW. A collection of breast cancer cell lines for the study of functionally distinct cancer subtypes. Cancer Cell. 2006; 10(6):515–527. doi:10.1016/j.ccr.2006.10.008. [PubMed: 17157791]
10. Lehmann BD, Bauer JA, Chen X, Sanders ME, Chakravarthy AB, Shyr Y, Pietenpol JA. Identification of human triple-negative breast cancer subtypes and preclinical models for selection of targeted therapies. J Clin Invest. 2011; 121(7):2750–2767. doi:10.1172/JCI45014. [PubMed: 21633166]
11. Sousa B, Paredes J, Milanezi F, Lopes N, Martins D, Dufloth R, Vieira D, Albergaria A, Veronese L, Carneiro V, Carvalho S, Costa JL, Zeferino L, Schmitt F. P-cadherin, vimentin and CK14 for identification of basal-like phenotype in breast carcinomas: an immunohistochemical study. Histol Histopathol. 2010; 25(8):963–974. [PubMed: 20552547]
12. Rodriguez-Pinilla SM, Sarrio D, Honrado E, Moreno-Bueno G, Hardisson D, Calero F, Benitez J, Palacios J. Vimentin and laminin expression is associated with basal-like phenotype in both sporadic and BRCA1-associated breast carcinomas. J Clin Pathol. 2007; 60(9):1006–1012. doi:10.1136/jcp.2006.042143. [PubMed: 17105822]
13. Livasy CA, Karaca G, Nanda R, Tretiakova MS, Olopade OI, Moore DT, Perou CM. Phenotypic evaluation of the basal-like subtype of invasive breast carcinoma. Mod Pathol. 2006; 19(2):264–271. doi:10.1038/modpathol.3800528. [PubMed: 16341146]
14. Tsang JY, Au SK, Ni YB, Shao MM, Siu WM, Hui SW, Chan SK, Chan KW, Kwok YK, Chan KF, Tse GM. P-cadherin and vimentin are useful basal markers in breast cancers. Hum Pathol. 2013; 44(12):2782–2791. doi:10.1016/j.humpath.2013.07.029. [PubMed: 24139214]
15. D'Alfonso TM, Hannah J, Chen Z, Liu Y, Zhou P, Shin SJ. Axl receptor tyrosine kinase expression in breast cancer. J Clin Pathol. 2014; 67(8):690–696. doi:10.1136/jclinpath-2013-202161. [PubMed: 24904064]
16. Rahman M, Davis SR, Pumphrey JG, Bao J, Nau MM, Meltzer PS, Lipkowitz S. TRAIL induces apoptosis in triple-negative breast cancer cells with a mesenchymal phenotype. Breast Cancer Res Treat. 2009; 113(2):217–230. doi:10.1007/s10549-008-9924-5. [PubMed: 18266105]
17. Ashkenazi A. Targeting death and decoy receptors of the tumour-necrosis factor superfamily. Nat Rev Cancer. 2002; 2(6):420–430. doi:10.1038/nrc821. [PubMed: 12189384]
18. Ashkenazi A, Pai RC, Fong S, Leung S, Lawrence DA, Marsters SA, Blackie C, Chang L, McMurtrey AE, Hebert A, DeForge L, Koumenis IL, Lewis D, Harris L, Bussiere J, Koeppen H, Shahrokh Z, Schwall RH. Safety and antitumor activity of recombinant soluble Apo2 ligand. J Clin Invest. 1999; 104(2):155–162. doi:10.1172/JCI6926. [PubMed: 10411544]

19. Walczak H, Miller RE, Ariail K, Gliniak B, Griffith TS, Kubin M, Chin W, Jones J, Woodward A, Le T, Smith C, Smolak P, Goodwin RG, Rauch CT, Schuh JC, Lynch DH. Tumoricidal activity of tumor necrosis factor-related apoptosis-inducing ligand in vivo. Nat Med. 1999; 5(2):157–163. doi:10.1038/5517. [PubMed: 9930862]

20. Holland PM. Death receptor agonist therapies for cancer, which is the right TRAIL? Cytokine Growth Factor Rev. 2014; 25(2):185–193. doi:10.1016/j.cytogfr.2013.12.009. [PubMed: 24418173]

21. Younes A, Vose JM, Zelenetz AD, Smith MR, Burris HA, Ansell SM, Klein J, Halpern W, Miceli R, Kumm E, Fox NL, Czuczman MS. A Phase 1b/2 trial of mapatumumab in patients with relapsed/refractory non-Hodgkin's lymphoma. Br J Cancer. 2010; 103(12):1783–1787. doi: 10.1038/sj.bjc.6605987. [PubMed: 21081929]

22. Camidge DR, Herbst RS, Gordon MS, Eckhardt SG, Kurzrock R, Durbin B, Ing J, Tohnya TM, Sager J, Ashkenazi A, Bray G, Mendelson D. A phase I safety and pharmacokinetic study of the death receptor 5 agonistic antibody PRO95780 in patients with advanced malignancies. Clin Cancer Res. 2010; 16(4):1256–1263. doi:10.1158/1078-0432.ccr-09-1267. [PubMed: 20145186]

23. Herbst RS, Eckhardt SG, Kurzrock R, Ebbinghaus S, O'Dwyer PJ, Gordon MS, Novotny W, Goldwasser MA, Tohnya TM, Lum BL, Ashkenazi A, Jubb AM, Mendelson DS. Phase I dose-escalation study of recombinant human Apo2L/TRAIL, a dual proapoptotic receptor agonist, in patients with advanced cancer. J Clin Oncol. 2010; 28(17):2839–2846. doi:10.1200/jco.2009.25.1991. [PubMed: 20458040]

24. von Pawel J, Harvey JH, Spigel DR, Dediu M, Reck M, Cebotaru CL, Humphreys RC, Gribbin MJ, Fox NL, Camidge DR. Phase II Trial of Mapatumumab, a Fully Human Agonist Monoclonal Antibody to Tumor Necrosis Factor-Related Apoptosis-Inducing Ligand Receptor 1 (TRAIL-R1), in Combination With Paclitaxel and Carboplatin in Patients With Advanced Non-Small-Cell Lung Cancer. Clin Lung Cancer. 2014; 15(3):188–196. e182. doi:10.1016/j.cllc.2013.12.005. [PubMed: 24560012]

25. Trarbach T, Moehler M, Heinemann V, Kohne CH, Przyborek M, Schulz C, Sneller V, Gallant G, Kanzler S. Phase II trial of mapatumumab, a fully human agonistic monoclonal antibody that targets and activates the tumour necrosis factor apoptosis-inducing ligand receptor-1 (TRAIL-R1), in patients with refractory colorectal cancer. Br J Cancer. 2010; 102(3):506–512. doi:10.1038/sj.bjc.6605507. [PubMed: 20068564]

26. Adams C, Totpal K, Lawrence D, Marsters S, Pitti R, Yee S, Ross S, Deforge L, Koeppen H, Sagolla M, Compaan D, Lowman H, Hymowitz S, Ashkenazi A. Structural and functional analysis of the interaction between the agonistic monoclonal antibody Apomab and the proapoptotic receptor DR5. Cell Death Differ. 2008; 15(4):751–761. doi:10.1038/sj.cdd.4402306. [PubMed: 18219321]

27. Murrow LM, Garimella SV, Jones TL, Caplen NJ, Lipkowitz S. Identification of WEE1 as a potential molecular target in cancer cells by RNAi screening of the human tyrosine kinome. Breast Cancer Res Treat. 2010; 122(2):347–357. doi:10.1007/s10549-009-0571-2. [PubMed: 19821025]

28. Garimella SV, Rocca A, Lipkowitz S. WEE1 inhibition sensitizes basal breast cancer cells to TRAIL-induced apoptosis. Mol Cancer Res. 2012; 10(1):75–85. doi: 10.1158/1541-7786.MCR-11-0500. [PubMed: 22112940]

29. Cohen GM. Caspases: the executioners of apoptosis. Biochem J. 1997; 326:1–16. Pt 1. [PubMed: 9337844]

30. Duriez PJ, Shah GM. Cleavage of poly(ADP-ribose) polymerase: a sensitive parameter to study cell death. Biochem Cell Biol. 1997; 75(4):337–349. [PubMed: 9493956]

31. Guarino M, Rubino B, Ballabio G. The role of epithelial-mesenchymal transition in cancer pathology. Pathology. 2007; 39(3):305–318. doi:10.1080/00313020701329914. [PubMed: 17558857]

32. Meric F, Lee WP, Sahin A, Zhang H, Kung HJ, Hung MC. Expression profile of tyrosine kinases in breast cancer. Clin Cancer Res. 2002; 8(2):361–367. [PubMed: 11839650]

33. Hong J, Belkhiri A. AXL mediates TRAIL resistance in esophageal adenocarcinoma. Neoplasia. 2013; 15(3):296–304. [PubMed: 23479507]

34. Miller LD, Smeds J, George J, Vega VB, Vergara L, Ploner A, Pawitan Y, Hall P, Klaar S, Liu ET, Bergh J. An expression signature for p53 status in human breast cancer predicts mutation status,

transcriptional effects, and patient survival. Proc Natl Acad Sci U S A. 2005; 102(38):13550–13555. doi:10.1073/pnas.0506230102. [PubMed: 16141321]

35. Pawitan Y, Bjohle J, Amler L, Borg AL, Egyhazi S, Hall P, Han X, Holmberg L, Huang F, Klaar S, Liu ET, Miller L, Nordgren H, Ploner A, Sandelin K, Shaw PM, Smeds J, Skoog L, Wedren S, Bergh J. Gene expression profiling spares early breast cancer patients from adjuvant therapy: derived and validated in two population-based cohorts. Breast Cancer Res. 2005; 7(6):R953–964. doi:10.1186/bcr1325. [PubMed: 16280042]
36. Wang Y, Klijn JG, Zhang Y, Sieuwerts AM, Look MP, Yang F, Talantov D, Timmermans M, Meijer-van Gelder ME, Yu J, Jatkoe T, Berns EM, Atkins D, Foekens JA. Gene-expression profiles to predict distant metastasis of lymph-node-negative primary breast cancer. Lancet. 2005; 365(9460):671–679. doi:10.1016/S0140-6736(05)17947-1. [PubMed: 15721472]
37. Berclaz G, Altermatt HJ, Rohrbach V, Kieffer I, Dreher E, Andres AC. Estrogen dependent expression of the receptor tyrosine kinase axl in normal and malignant human breast. Annals of oncology : official journal of the European Society for Medical Oncology / ESMO. 2001; 12(6): 819–824. [PubMed: 11484958]
38. Popnikolov NK, Ayala AG, Graves K, Gatalica Z. Benign myoepithelial tumors of the breast have immunophenotypic characteristics similar to metaplastic matrix-producing and spindle cell carcinomas. American journal of clinical pathology. 2003; 120(2):161–167. doi:10.1309/G6CT-R8MD-TFUW-19XV. [PubMed: 12931544]
39. Wilson NS, Yang B, Yang A, Loeser S, Marsters S, Lawrence D, Li Y, Pitti R, Totpal K, Yee S, Ross S, Vernes JM, Lu Y, Adams C, Offringa R, Kelley B, Hymowitz S, Daniel D, Meng G, Ashkenazi A. An Fcgamma receptor-dependent mechanism drives antibody-mediated target-receptor signaling in cancer cells. Cancer Cell. 2011; 19(1):101–113. doi:10.1016/j.ccr.2010.11.012. [PubMed: 21251615]
40. Truneh A, Sharma S, Silverman C, Khandekar S, Reddy MP, Deen KC, McLaughlin MM, Srinivasula SM, Livi GP, Marshall LA, Alnemri ES, Williams WV, Doyle ML. Temperature-sensitive differential affinity of TRAIL for its receptors. DR5 is the highest affinity receptor. J Biol Chem. 2000; 275(30):23319–23325. doi:10.1074/jbc.M910438199. [PubMed: 10770955]
41. Rahman M, Pumphrey JG, Lipkowitz S. The TRAIL to targeted therapy of breast cancer. Adv Cancer Res. 2009; 103:43–73. doi:10.1016/S0065-230X(09)03003-6. [PubMed: 19854352]
42. Wagner KW, Punnoose EA, Januario T, Lawrence DA, Pitti RM, Lancaster K, Lee D, von Goetz M, Yee SF, Totpal K, Huw L, Katta V, Cavet G, Hymowitz SG, Amler L, Ashkenazi A. Death-receptor O-glycosylation controls tumor-cell sensitivity to the proapoptotic ligand Apo2L/TRAIL. Nat Med. 2007; 13(9):1070–1077. doi:10.1038/nm1627. [PubMed: 17767167]
43. Lu M, Marsters S, Ye X, Luis E, Gonzalez L, Ashkenazi A. E-cadherin couples death receptors to the cytoskeleton to regulate apoptosis. Mol Cell. 2014; 54(6):987–998. doi:10.1016/j.molcel.2014.04.029. [PubMed: 24882208]
44. Ashkenazi A. Targeting the extrinsic apoptotic pathway in cancer: lessons learned and future directions. J Clin Invest. 2015; 125(2):487–489. doi:10.1172/JCI80420. [PubMed: 25642709]
45. Prat A, Parker JS, Karginova O, Fan C, Livasy C, Herschkowitz JI, He X, Perou CM. Phenotypic and molecular characterization of the claudin-low intrinsic subtype of breast cancer. Breast Cancer Res. 2010; 12(5):R68. doi:10.1186/bcr2635. [PubMed: 20813035]
46. Chavez KJ, Garimella SV, Lipkowitz S. Triple negative breast cancer cell lines: one tool in the search for better treatment of triple negative breast cancer. Breast disease. 2010; 32(1-2):35–48. doi:10.3233/BD-2010-0307. [PubMed: 21778573]
47. Carey LA, Dees EC, Sawyer L, Gatti L, Moore DT, Collichio F, Ollila DW, Sartor CI, Graham ML, Perou CM. The triple negative paradox: primary tumor chemosensitivity of breast cancer subtypes. Clin Cancer Res. 2007; 13(8):2329–2334. doi:10.1158/1078-0432.CCR-06-1109. [PubMed: 17438091]
48. Willipinski-Stapelfeldt B, Riethdorf S, Assmann V, Woelfle U, Rau T, Sauter G, Heukeshoven J, Pantel K. Changes in cytoskeletal protein composition indicative of an epithelial-mesenchymal transition in human micrometastatic and primary breast carcinoma cells. Clin Cancer Res. 2005; 11(22):8006–8014. doi:10.1158/1078-0432.CCR-05-0632. [PubMed: 16299229]
49. Keane MM, Ettenberg SA, Nau MM, Russell EK, Lipkowitz S. Chemotherapy augments TRAIL-induced apoptosis in breast cell lines. Cancer Res. 1999; 59(3):734–741. [PubMed: 9973225]

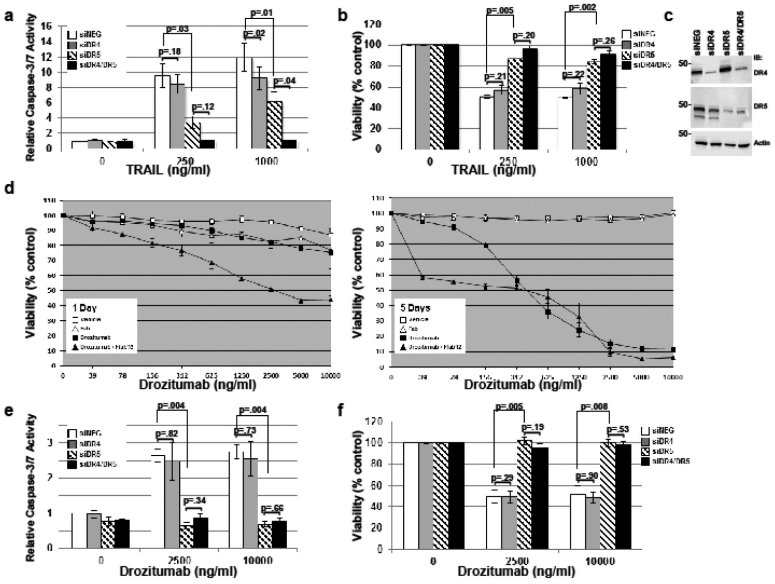

Fig. 1. Drozitumab induces loss in viability via DR5

(a-c). MB231 cells were transfected with a nontargeting siRNA (siNEG), an siRNA for DR4 (siDR4), and siRNA for DR5 (siDR5), or an siRNA for both DR4 and DR5 (siDR4/DR5). 48 h after transfection, cells were treated with GST-TRAIL at the indicated concentrations and (a) caspase-3 and -7 activity was measured using the Caspase-Glo® 3/7 assay 1 h post GST-TRAIL addition and represents relative activity compared to siNEG transfected untreated cells (b) viability was measured by MTS assay at 72 h post GST-TRAIL addition and represents viability normalized to siNEG transfected, untreated cells. (c) Representative immunoblot showing knockdown of DR4 and DR5. (d) MB231 cells were incubated with indicated doses of drozitumab vehicle, drozitumab vehicle plus 10 ug/mL F(ab')2, drozitumab, or drozitumab plus 10 ug/mL F(ab')2 for 1 and 5 days (left and right panels, respectively). Viability was assessed using the MTS assay. Data were normalized to the no treatment vehicle control. (e-f) The siRNA transfected MB231 cells used in panel a and b were treated with drozitumab + F(ab')2 48 h after transfection and (d) caspase-3 and -7 activity was measured 24 hours post drozitumab addition using the Caspase-Glo® 3/7 assay and represents relative activity compared to siNEG transfected untreated cells (f) viability was measured by MTS assay at 72 hours post drozitumab addition and represents data normalized to siNEG transfected, untreated cells. Viability and caspase activity represent three experiments +/− SE. p values shown were calculated using a paired, two tailed Student's t-test.

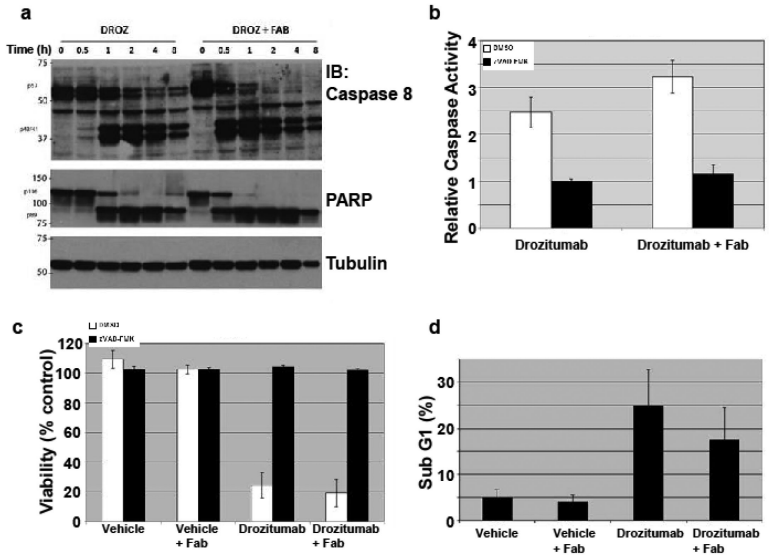

Fig. 2. Drozitumab-induced cell death is caspase dependent apoptosis

(a) MB231 cells were incubated with drozitumab or drozitumab plus 10 μg/ml F(ab')2 until cells were harvested for protein isolation at the indicated time points (hours). Immunoblot analysis was used to characterize caspase-8 and PARP cleavage. Tubulin was used as a loading control. (b) MB231 cells were pre-treated with vehicle or the pan-caspase inhibitor ZVAD-FMK (100 uM) for 2 hours and subsequently treated overnight with drozitumab or drozitumab plus F(ab')2. Caspase-3 and -7 activity was subsequently measured using Caspase-Glo® 3/7 assay system. (c) Cells were treated as in 2b, with the addition of drozitumab vehicle and drozitumab vehicle plus F(ab')2. Cells were subsequently incubated for 5 days before viability was assessed via MTS assay. (d) MB231 cells were treated with 10 ug/mL drozitumab vehicle, drozitumab vehicle plus F(ab')2, drozitumab, and drozitumab plus F(ab')2 for two days. Cells were stained with propidium iodide and underwent FACS analysis to assess sub-G1 DNA content. All data were normalized to the treatment control for each experiment and are the average of three experiments +/− SE.

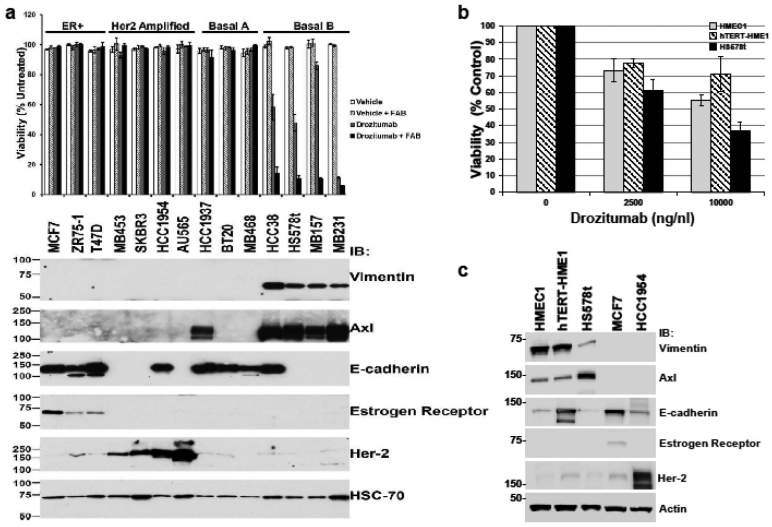

Fig. 3. TNBC cells express vimentin and Axl

(a) A panel of breast cancer cell lines representative of the different subtypes of disease were treated with drozitumab vehicle; drozitumab vehicle plus F(ab')2; 10 ug/mL drozitumab; and 10ug/mL drozitumab plus F(ab')2 for 5 days. Viability was then measured by MTS assay, and cells were harvested for immunoblotting to assess the expression of subtype markers. All data were normalized to the treatment control for each experiment and are the average of three experiments +/− SE. (b) Non-transformed mammary epithelial cells (HMEC1 and hTERT-HME1) where treated with drozitumab + F(ab')2 at the indicated concentrations and viability was measured using an MTS assay at 72 h. (c) Expression of protein markers were assessed in the non-transformed cell lines by immunoblot using the indicated antibodies. The HS578t (TNBC, vimentin and Axl positive), MCF7 (ER+, E-cadherin positive), and HCC1954 (Her-2 amplified, Her-2 and E-cadherin positive cell lines were included on the immunoblot as controls for the different antibodies as indicated). MW in kDa is shown to the right of the panels.

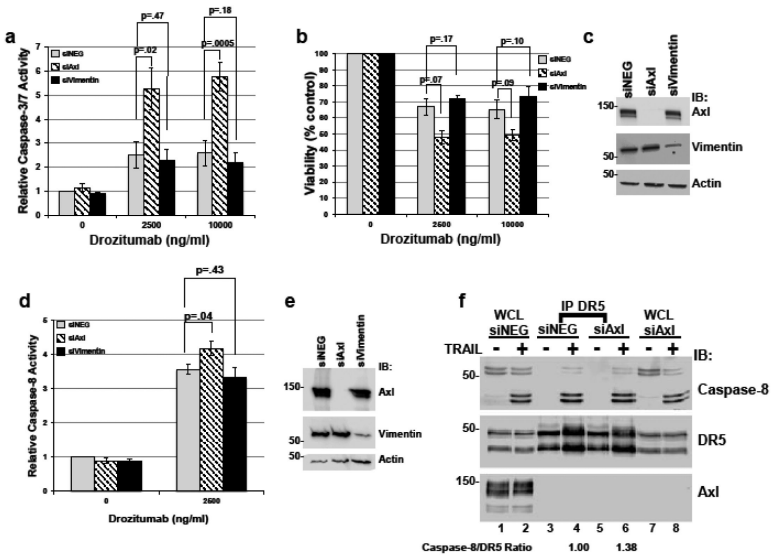

Fig. 4. Axl negatively regulated drozitumab induced caspase activation and loss of viability

Cells were transfected with a nontargeting siRNA pool (siNEG), an siRNA pool targeting Axl (siAxl), or an siRNA pool targeting vimentin (siVimentin) as indicated. (a) Drozitumab +F(ab')2 induced caspase-3 and -7 activity was measured after 24 hours or (b) drozitumab +F(ab')2 induced loss of viability was measured at 72 h. (c) Representative immunoblot showing knockdown of Axl and vimentin. (d) Caspase-8 activity was measured in the siRNA transfected cells using a Caspase-Glo® 8 assay system. (e) Representative immunoblot showing knockdown of Axl and vimentin. (f) DR5 was immunoprecipitated from cells treated with or without drozitumab as described in the Materials and Methods section and caspase-8 recruitment to DR5 was analyzed by immunoblotting. Lanes 1 and 2, and lanes 7 and 8 show the whole cell lysates (WCL) for siNEG and siAxl, respectively. The antibodies used are shown to the right of the blots and MW in kDa is listed to the left. The ratio of caspase-8/DR5 in the DR5 immunoprecipitates is shown below the blot (lanes 4 and 6) normalized to the ratio of the siNEG lane.

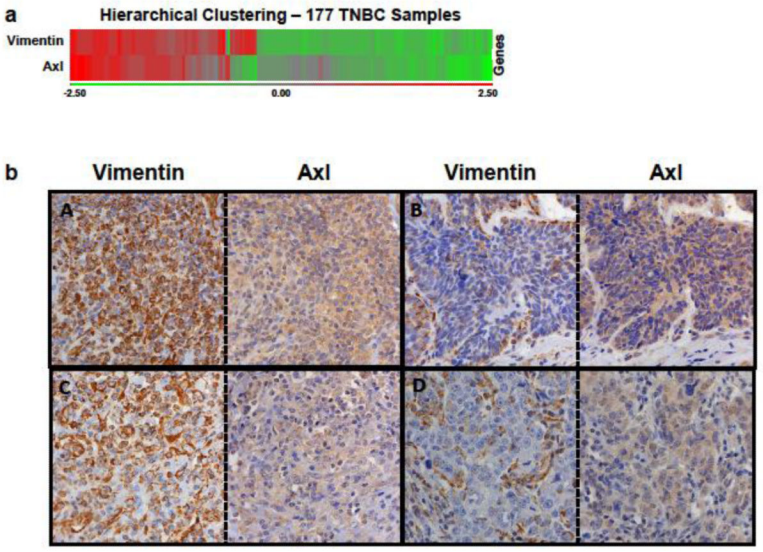

Fig. 5. TNBC tumors expresses vimentin and Axl

(a) Heatmap displaying expression of vimentin and Axl for hierarchically clustered 177 TNBC samples. (b) Representative IHC images of the four patterns of vimentin and Axl staining observed. A) High vimentin, high Axl, B) Low vimentin, high Axl, C) High vimentin, low Axl, and D) Low vimentin, low Axl. Vimentin image right, Axl image left. All images 450X magnification.

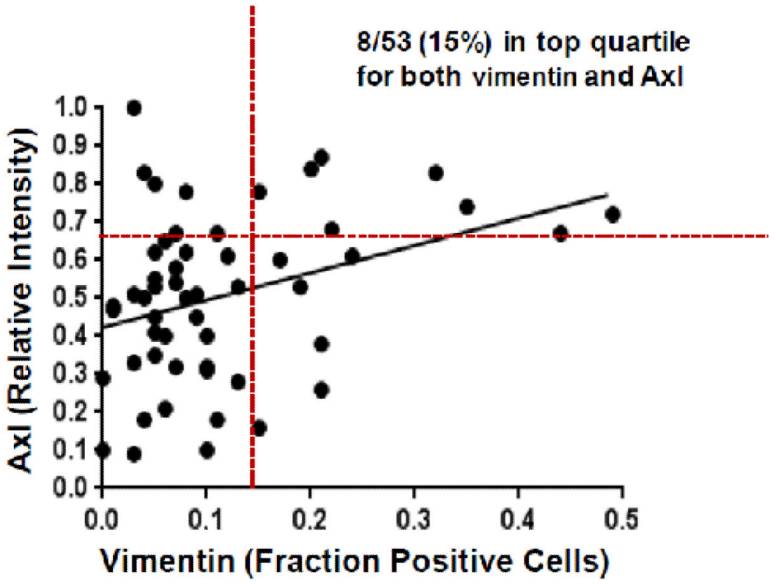

Fig. 6. Vimentin and Axl are co-expressed in TNBC

The vertical red dotted line indicates the top quartile for vimentin staining and the horizontal red dotted line indicates the top quartile for Axl staining.

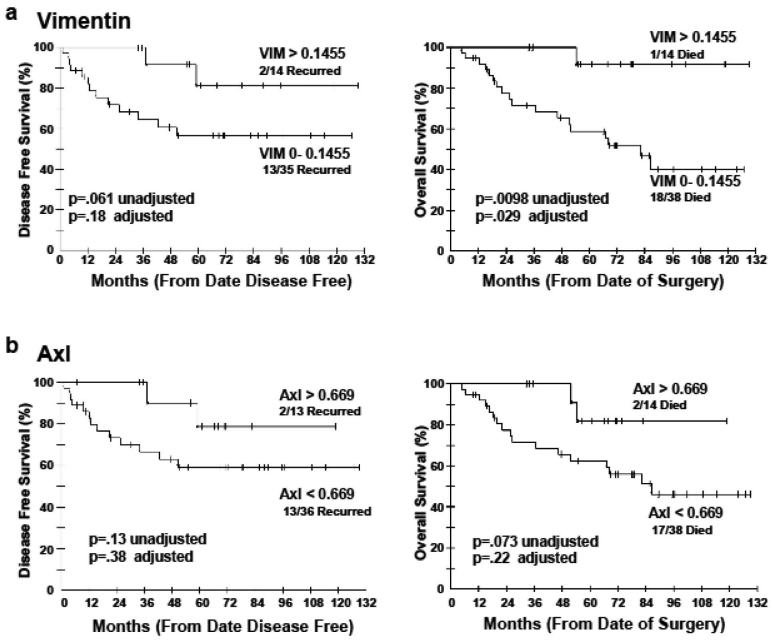

Fig. 7. Kaplan-meier curves for Vimentin and Axl expressioin and DFS (left panels), and OS right panels)

(a) DFS and OS survival based on high vs. low vimentin expression by IHC. (b) DFS and OS survival based on high vs. low Axl expression by IHC.

Table 1

Characteristic	Number & percentage
Stage at diagnosis (n= 53)	
Stage 1	6 (11.3%)
Stage 2	30 (56.6%)
Stage 3	16 (30.1%)
Stage 4	1 (1.88%)
Type of surgery	
Breast conserving	33 (62.2%)
Mastectomy	19 (35.84%)
Unknown	1 (0.01%)
Chemotherapy	
Yes	50 (94.33%)
No	3 (5.66%)
Type of chemotherapy	
Neoadjuvant	21 (42.0%)
Adjuvant	29 (58.0%)
Response to neoadjuvant chemotherapy (n = 21)	
Pathological complete response (PCR)	2 (9.52%)
Residual disease	16 (76.19%)
Progressed	3 (14.28%)
Completed chemotherapy	
Yes	33 (66.0%)
No	16 (32.0%)
Unknown	1 (2.0%)
Disease recurrence	
Yes	35 (66.03%)
No	18 (33.96%)

Table 2

A

Multivariable Cox proportional hazards model for DFS

Parameter	p-value	Hazard Ratio	95% Hazard Ratio Confidence Limits
Vim >0.1455	0.046	0.210	0.046-.970
Age >55	0.016	0.234	0.072-.764
Stage	0.0004	7.555	2.486-22.960

Vimentin>0.1455 was shown to be associated with superior DFS when adjusting for age and stage.

B

Multivariable Cox proportional hazards model for OS

Parameter	p-value	Hazard Ratio	95% Hazard Ratio Confidence Limits
Vim >0.1455	0.026	0.101	0.013-.762
Stage	0.016	3.192	1.244-8.191

Vimentin>0.1455 was associated with lower probability of dying when adjusting for other potential prognostic factors.